Case Studies in Construction Materials 17 (2022) e01334

Contents lists available at ScienceDirect

Case Studies in Construction Materials

journal homepage: www.elsevier.com/locate/cscm

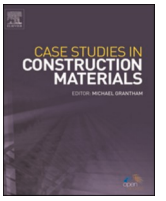

Case study

Structural use of fiber-reinforced self-compacting concrete with recycled aggregates: Case study of a foundation wall in Spain

Jose A. Ortiz-Lozano [a,*], Francisco Mena-Sebastia [b], Ignacio Segura [b], Albert de la Fuente [b], Antonio Aguado [b]

[a] Department of Construction and Structures. Universidad Autónoma de Aguascalientes, Mexico
[b] Department of Civil and Environmental Engineering. Universitat Politècnica de Catalunya, UPC Tech, Spain

ARTICLE INFO

Keywords:
Fiber-reinforced concrete
Recycled aggregates
Toughness
Self-compacting concrete
Full-scale test

ABSTRACT

This paper is focused on the use of mixed recycled-aggregates (RA), replacing 100% of the natural coarse aggregates, for producing steel fiber reinforced self-compacting concrete (FR-SCC-RA) oriented to the construction of foundation walls. To this end, an extensive experimental program dedicated to the mechanical characterization of FR-SCC-RA foundation walls from the material and structural level was carried out. The former was developed on both molded specimens and cores extracted from the in-situ constructed FR-SCC-RA walls in Barcelona, Spain. The results lead to confirm that the use of RA resulted satisfactorily from both the concrete manufacturing and the mechanical performance, since no affectations on the design mechanical variables (i.e., compressive and flexural tensile strengths) were detected. Likewise, the results derived from the full-scale test evidenced that the residual loads of the slabs tested were significantly higher than those calculated based on the test results of the prismatic core samples. The main outcome derived from the experimental research program is that FR-SCC-RA might be a suitable material for this structural typology and that the tested slabs presented a sufficient post-cracking residual capacity -due to the incorporation of structural fibers- for avoiding fragile failures. These conclusions could be extended to other countries where similar restrictive regulations and standards are present, regarding the use of RA and FRC for structural applications.

1. Introduction

The use of recycled aggregates (RA) for producing concrete is often limited the regulations and standards applicable in each country. In some cases, mixed recycled aggregates are allowed only in non-structural applications such as filling of trenches or road sub-bases [1–4]. Consequently, the reuse for concrete production of the construction and demolition waste generated is partially valorized, this leading to a reduction of the sustainability performance of the construction sector [5–7]. Therefore, there are still many improvement opportunities in this regard.

In Spain, approximately 70% of the RA is composed of clean aggregate and bonded mortar. Usually, the amount of impurities in the aggregates far exceeds the limits required by Structural Code 2021 [6]. A clear example of this is the content of ceramic material: while its mean value in the analyzed samples [8] is 22%, the maximum value currently allowed is just 5%.

* Correspondence to: Department of Civil Engineering Autonomous University of Aguascalientes, Ciudad Universitaria, Av. Universidad, 940 (module 108), C.P. 20100 Aguascalientes, Mexico.
E-mail address: jose.ortiz@edu.uaa.mx (J.A. Ortiz-Lozano).

https://doi.org/10.1016/j.cscm.2022.e01334
Received 4 September 2021; Received in revised form 20 June 2022; Accepted 20 July 2022
Available online 22 July 2022

Moreover, the properties of RA are different from those of natural aggregates (NAs), and in the case of mixed or ceramic RA the differences are more evident. The characterization of a RA usually focuses on three aspects: *composition*, *density*, and *water absorption*. Those have influence on both the fresh and hardened properties of the resulting concrete.

Regarding the *composition*, there is an increasing linear relationship between ceramic material content and the increase in water absorption and in the Los Angeles abrasion coefficient. This phenomenon is due to the greater porosity and fragility of ceramic materials compared to natural stone [9]. Additionally, most RAs satisfy the fragmentation resistance requirement.

Previous studies [10,11] have shown that, unlike NAs for which *absorption* is fast and barely significant (approximately 0.5–1.0%), in RAs it lasts beyond 24 h and can end after 96–120 h. This can be simulated with a function that reproduces the phenomenon under different conditions of the origin of the aggregate [12]. The absorption recorded at 24 h represents between 60% and 70% of its maximum capacity. In addition, the absorption of water during the first 5–10 min represents between 75% and 85% of the absorption at 24 h [12]. Due to this, to avoid loss of concrete workability, there are different approaches: (1) provide additional water, (2) pre-saturate or wash the RAs [13], (3) acid treatment [14] or (4) treatment with absorption-inhibitor additive.

Other studies [15–17], dealing with pervious or porous concrete for pavements incorporating RAs as well as fibers and mineral additives, have found that using RAs decreased density and strength (compressive and flexural), increased void content and permeability of concrete. Nevertheless, recycled ceramic aggregates have been used as internal curing materials for high performance concrete (HPC) [18], these resulting highly efficient in reducing autogenous shrinkage of HPC while maintaining a satisfactory level of mechanical properties.

Moreover, from a mechanical standpoint, if the substitution is limited to 20% by weight of the coarse aggregate content, the strength of the concrete is hardly affected compared to that of conventional concrete [6,19]. For higher substitution percentages, there is generally a reduction in the mechanical properties of the concrete, which depends on the properties and type of RA. In this regard, compressive strength of bricks (3–7 MPa) is up to 40 times lower than that of a natural rock (70–280 MPa), as the main source of aggregate [20].

Previous studies have shown that in concretes with high **w/c** ratios greater than 0.55, the compressive strength of concrete ($\boldsymbol{f_c}$) with RAs is similar to that of a conventional concrete, even with 100% of substitution [21]. However, as the **w/c** ratio decreases, the differences in $\boldsymbol{f_c}$ between both types of concrete increase, these reaching 25% for **w/c** ratios = 0.40.

In this regard, [22] reports a 20–25% reduction in $\boldsymbol{f_c}$ when coarse aggregates are completely substituted with recycled concrete aggregate (RCA), through a pre-saturation process of aggregates, for the same **w/c** ratio (equal to 0.50) and a cement dosage of 325 kg/m^3.

In case of 25% and 50% substitution of natural sand with fine sand RAs (using 100% coarse recycled aggregate in all cases), [23] obtain comparable values of $\boldsymbol{f_c}$, but it is required to make a compensation in order to reduce loss of workability. For higher substitution percentages, between 75% and 100%, the strength reduction is 10.1% and 11.3%, respectively. [24] attribute the good strength performance of fine ceramic RA to a better binding capacity produced by pozzolanic chemical reactions, combined with internal curing initiated by the reserve of water absorbed through the manufacture of concrete.

The effect of RA on the modulus of elasticity ($\mathbf{E_c}$) is greater than on other mechanical properties. First, the deformability of the mixed RA with respect to the NA is greater, and second, a weaker connection between the old and the new aggregate-paste interphase, with a larger net of capillary pores and microcracks. Consequently, the substitution of all the coarse fraction with RA has negative effects on this property. Specifically, the use of RA (in the case of a 100% substitution of the coarse fraction) leads to a reduction of $\mathbf{E_c}$ ranging between 15% and 48% $\mathbf{E_c}$ [22,25–28]. The Poisson's ratio for concrete with RA ranges between 0.14 and 0.20, regardless of the substitution ratio [29], which represents a reduction of up to 30% compared to conventional concrete.

In Spain, article 30.8.1 of the Structural Code 2021 [6], about using recycled aggregates regulates the use of RA for producing concrete with structural purposes. In this article, the maximum substitution percentage is limited to 20% of the coarse fraction as long as the aggregate is obtained from crushed concrete and the water absorption is minor than 7%. However, [6] allows for a higher percentage of substitution provided the performance of the resulting concrete is qualified based on particular studies and complementary testing.

The replacement levels established in the regulations are often generic, and these can be restrictive for some structural applications. This is the case, for instance, of in-situ pile caps or other foundation elements, where these limits could be exceeded to improve both the mechanical and sustainability performance [7]. Moreover, for this type of structural typologies, self-compactability and steel fiber reinforcement (replacing the traditional steel reinforcement), can be added to achieve a higher degree of economic-technical competitiveness [30].

Concrete self-compactability allows reducing the likelihood of discontinuities or voids [31], construction time, noise and vibrations since compaction tasks are eliminated. These have a positive effect on economic, environmental and social indicators as it has been proven for several FR-SCC structural components. In this regard, sustainability-oriented analyses in which the positive outcomes derived from the use of SCC (and fibers) [32–34] for precast segmental tunnel linings and pile-supported flat-slabs are presented in [35] and [36], respectively.

Besides, the use of steel fibers (in total [37] or partial substitution of the steel bars) can be suitable in (1) lightly-reinforced structures for which only a minimum skin reinforcement is required and, consequently, this could be replaced by a competitive amount of fibers [15,16,38–41] and (2) when the placement of the reinforcement cage is complex or time consuming, such as on slabs [42–44], tunnel linings [45], pipelines [46] and in walls [47] and piles for foundations [30].

So far, a great number of experimental programs on full-scale testing FRC beam and slab-type elements were carried out and reported in the literature [48–54]. These experimental programs have evidenced that the use of structural fibers as bending reinforcement and in shear behavior [55,56] is of technical and economic interest, and these have allowed significant advances in terms of

Table 1
Contents for the different concrete dosages (kg/m^3).

Component	NA/SCC 12	RA/SCC 20	RA/SCC 20 +I	FR-RA/12–35a	FR-RA/SCC 12–35b	FR-RA/SCC 20–50
Cement CEM II/A-M (V-L) 42.5 R	355	370	370	370	370	370
0/4-T-L	1230	1210	1210	1240	1260	1260
6/12-T-L	580	–	–	–	–	–
4/12-T-R	–	180	200	540	520	180
Agg. without mortar		*97*	*108*	291	*280*	*97*
Agg. with mortar		*51*	*57*	153	*147*	*51*
Ceramic		*11*	*12*	32	*31*	*11*
Saturation water		*18*	*20*	54	*52*	*18*
Others (glass, wood, etc.*)*		*3*	*3*	10	*9*	*3*
12/20-T-R	–	360	390	–	–	340
Agg. without mortar		*151*	*168*			*142*
Agg. with mortar		*111*	*123*			*104*
Ceramic		*50*	*56*			*47*
Saturation water		*36*	*39*			*34*
Others (glass, wood, etc.*)*		*12*	*13*			*11*
M502 fibers	–	–	–	–	–	20
M503 fibers	–	–	–	20	20	–
Water	170	150	170	170	175	160
Inhibition admixture	–	–	1.5	–	–	–
Lignosulphonate	2.2	2.2	2.6	2.6	2.6	2.6
Polycarboxylate	6.8	6.8	6.8	7.3	7.3	7.3
Total	2344	2279	2351	2350	2355	2340
Fines	548.4	567.4	568.7	581.5	583.7	574.5
Effective w/c ratio	0.479	0.405	0.459	0.459	0.473	0.432
Volume (m^3)	3	6	6	6	6	6

design. However, to the best authors' knowledge, none of those contemplated the use of RA.

Based on the abovementioned, the objective of this paper is to present and discuss the results obtained from an extensive experimental program oriented to characterize the mechanical performance of FR-SCC-RA full-scale slabs subjected to bending. These slabs were obtained from sawing a wall foundation produced with this material, which was previously designed and characterized at the laboratory facilities [57]. The results and subsequent analysis presented herein allow reinforcing the suitability of this innovative material for this type of applications. This, however, should be seen as a case study and there are still several points related to standardization, characterization and design aspects that have to be dealt with further research.

2. Experimental program

A total of six types of batches of Self-Compacting Concrete made with Recycled Aggregates and Reinforced with Steel Fibers (FR-SCC-RA) were produced.

The concretes were manufactured in a concrete batching plant in Barcelona (Spain), where moulded specimens were made for the physical and mechanical characterization of the concrete. The results obtained as well as the procedures for mixing and manufacturing the control specimens can be found in [57]. In the same reference, the characterization in fresh state results is also reported and analyzed.

2.1. SRF-SCC-RA mix proportions and materials

The cement used for producing concrete was CEM II/A-M (V-L) 42.5 R. The aggregates were limestones of 6–12 mm and 0–4 mm particle sizes: 6/12-T-L and 0/4-T-L, respectively. Furthermore, two varieties of recycled aggregates were used: 4–12 mm (4/12-T-R) and 12–20 mm (12/20-T-R) particle size. The recycled aggregates used consisted of ceramics, clean aggregate particles, mortar, and some other minor components such as organic matter, plaster, glass and wood, among others. The nomenclature used was as follows: 'T' aggregate originated by trituration, 'L' limestone origin and 'R' recycled origin. The composition and physical properties of the recycled aggregates used in this study, can be consulted in [57].

Two types of hooked-end steel fibers were used: M502 (length of 50 mm) and M503 (length of 35 mm); the geometrical and mechanical properties of these fibers are presented in [57]. A dosage of 20 kg/m^3 was added to assure a minimal ductility as well as sufficient post-cracking strength to prevent the slabs from brittle failure [58,59]; this lowest reinforcing quantity is suggested in the EHE-08 [6] for elements with small structural relevance.

A superplasticizer (polycarboxylate), a plasticizer (lignosulfonate) and an admixture able to prevent the water absorption in recycled aggregates, as an alternative to water pre-saturation, were used for producing the concretes.

Table 1 presents the FR-SCC-RA dosages for concrete. The terminology for the mixes is T/C MSA–l_f+I, where 'T' is the type of concrete ('NA' is natural coarse aggregate, 'RA' is recycled coarse aggregate, 'FRC-RA' is reinforced with fibers and recycled coarse aggregate); 'C' is consistency, 'SCC' is self-compacting (in all cases); 'MSA' is maximum aggregate size; 'l_f' is maximum fiber length (mm); and 'I' is the admixture for absorption inhibition [57].

(a)

(b)

(c)

Fig. 1. Construction procedure: a) Excavated trench, b) Thixotropic sludge, c) Concrete pouring from truck.

Due to the issues found during the process of mixing dosage FR-RA/12–35a (this sample is not considered as SCC), with difficulties in meeting the self-compacting requirements, that dosage was repeated (FR-RA/SCC 12–35b) with slight modifications to the granular skeleton, and consequently there are two concretes with that dosage.

2.2. Case study: Foundation wall in Barcelona (Spain)

A full-scale on-site pilot test was carried out in which the concrete produced was used to build six foundation walls using trenches, in order to subsequently analyze the physical and mechanical properties of test specimens extracted from the walls. The specimens were extracted from the work site and cut, to compare the results obtained from the core samples extracted from the walls built during the pilot test and the results from the samples produced in the concrete plant, which can be consulted in [57]. The concrete was transported by truck mixer to the testing section located at the work site. The travel distance was approximately 15 km and took approximately 20–30 min.

The construction procedure used in the pilot test consisted in the excavation of the trench with the established dimensions (3500

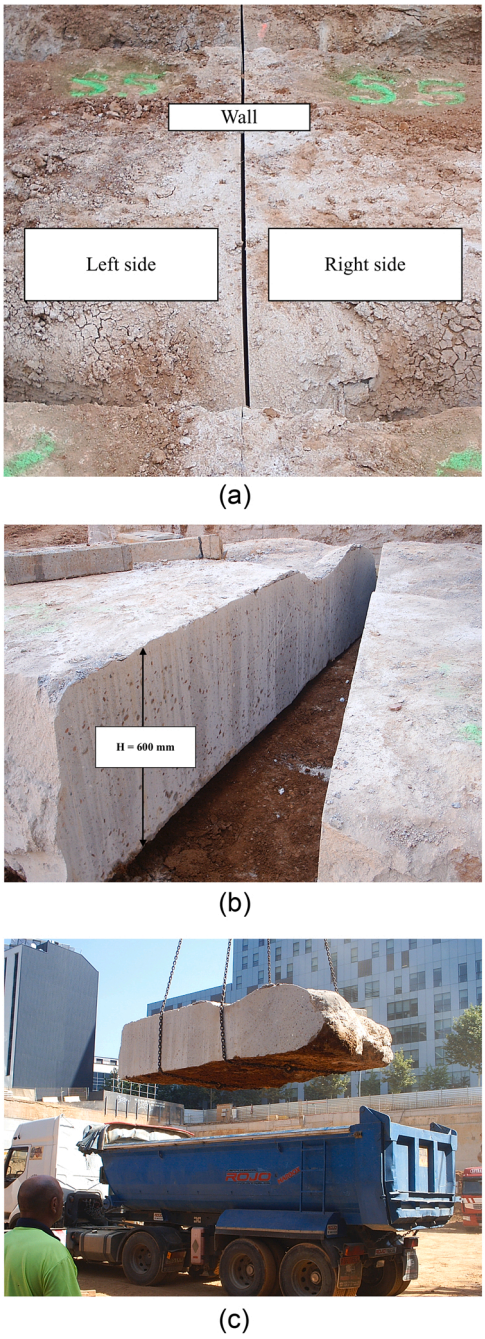

Fig. 2. a) and b) Cut applied, c) Handling and transport.

mm deep, 2500 mm long and 600 mm wide). Subsequently, the excavations are filled with thixotropic or bentonite mud to avoid possible collapse of the trenches.

The pouring of the concrete in the six foundation walls was carried out with the help of a chute, a bucket and a tremie pipe. The flow dynamics of the concrete deposited in the trench is determined by the boundary conditions used during the pouring [60,61]. In this manner, as the concrete fills the trench (from the bottom up), the excess sludge rises to the surface due to its lower density. Fig. 1 shows the different phases of the construction procedure.

A different type of concrete was poured in each foundation wall, for a total of six walls and six dosages, respectively: Wall 1 (RA/SCC 20), Wall 2 (FR-RA/SCC 12–35b), Wall 3 (NA/SCC 12), Wall 4 (RA/SCC 20 +I), Wall 5 (FR-RA/12–35a) and Wall 6 (FR-RA/SCC 20–50).

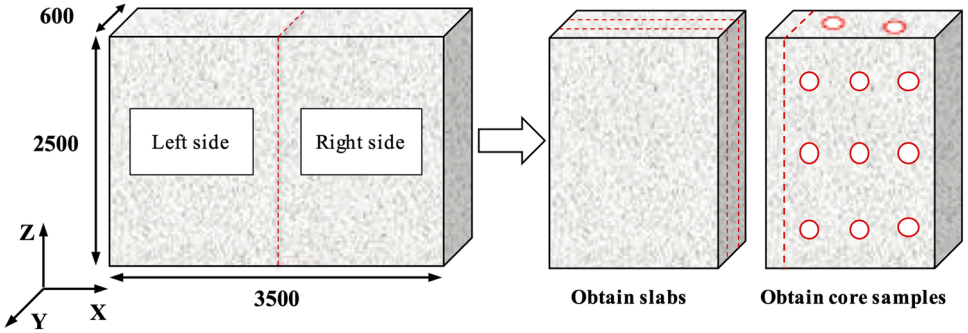

Fig. 3. Foundation wall cutting diagram (dimensions in mm).

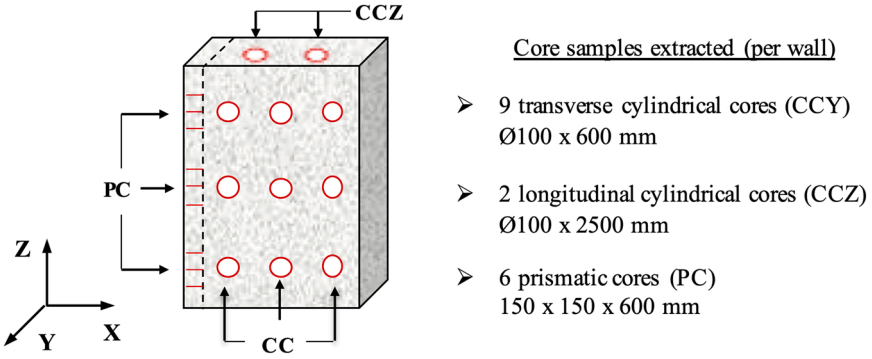

Fig. 4. Number and type of core samples extracted (per wall).

2.3. Core specimens cutting and extraction plan

2.3.1. Core specimen cutting plan

The six foundation walls built during the pilot test were extracted to carry out mechanical characterization studies on the full-scale structural elements. To transport the slabs to the laboratory, the six walls had to be cut lengthwise into two halves, as Fig. 2 shows, from which twelve pieces with approximate dimensions of 2500 mm × 1750 mm x 600 mm were obtained.

Since for each wall there were two pieces of similar dimensions available, two different lines of research were planned, one for each wall, as Fig. 3 shows:

1. Specimens cored (cylindrical, prismatic and cubic) to analyze the variability of physical and mechanical properties as a function of the 'Z' (vertical) dimension, and thus detect possible anomalies caused by the construction process, such as aggregates segregation, accumulation of fibers or presence of cracks.
2. Slabs for testing under a three-point bending configuration (flexural bending in isostatic conditions). It must be remarked that -owe to the variability of thickness- it was assumed that the degree of variability of the mechanical results would be high. Nonetheless, for the comparison of the different concretes, and to verify that the failure was not brittle, these elements and its geometry were found acceptable and representative of the real boundary conditions.

2.3.2. Extraction of core specimens

The core samples were extracted following the cutting plan described below. Fig. 4 details the number of core samples obtained for each wall, grouped according to their type, and shows the three types of core samples to extracted from each piece.

- 6 prismatic cores (PC) of 150×150×600 mm, grouped in pairs, making nine cuts on the previously obtained plate.
- longitudinal cylindrical cores (CCZ) 100 mm diameter and a length equal to the height of the wall 'L' (2200–2500 mm).
- 9 transverse cylindrical cores (CCY) 100 mm diameter and a length equal to the thickness of the wall 'H' (600 mm).

Fig. 5 shows some details of the extraction of the prismatic and cylindrical specimens from the extracted walls.

2.3.3. Cutting and producing the slabs

The slabs were extracted from the right half of each wall, and on each piece two longitudinal cuts were made, as Fig. 6 shows, using

(a)

(b)

(c)

Fig. 5. Obtaining the a) and b) prismatic and c) cylindrical core samples.

the diamond wire cutting technique.

From each piece, three slabs approximately 200 mm thick were obtained. The identification of each slab was made in Spanish according to its placement, the upper slab was marked with the letter "S", the central slab with "C" and the lower slab with an "I", as Fig. 7a shows. Once the cuts were completed, the slabs were transported by truck to the "Lluís Agulló" Structures Technology Laboratory (LTE for its initials in Spanish) of the Polytechnic University of Catalonia (Fig. 7b), to conduct the flexural tests.

2.4. Mechanical characterization tests

2.4.1. Core specimens extracted from the foundation walls

A total of 318 core samples were obtained, distributed as follows: 208 CCZ and CCY and 110 PC. Table 2 shows the test plan and the properties analyzed for each type of core sample, the standard or method applied, as well as the number of specimens tested.

The tests for the mechanical characterization: compressive strength (f_c), flexural tension ($f_{ct,fl}$), toughness (G_f) and modulus of elasticity (E_c), were performed by the aid of an Ibertest press of 3 MN of capacity, controlling the displacement.

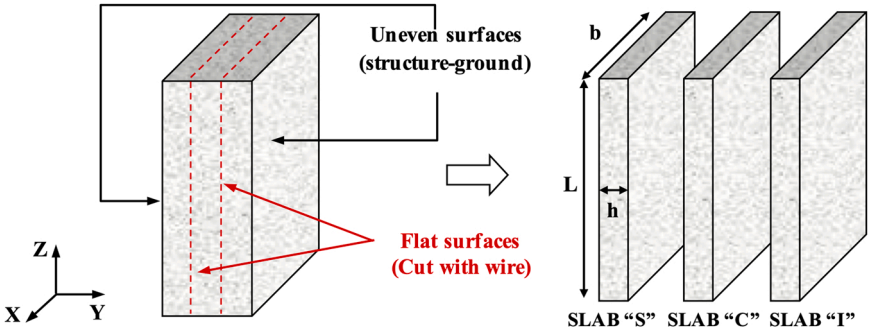

Fig. 6. Production of plates (left half of each wall).

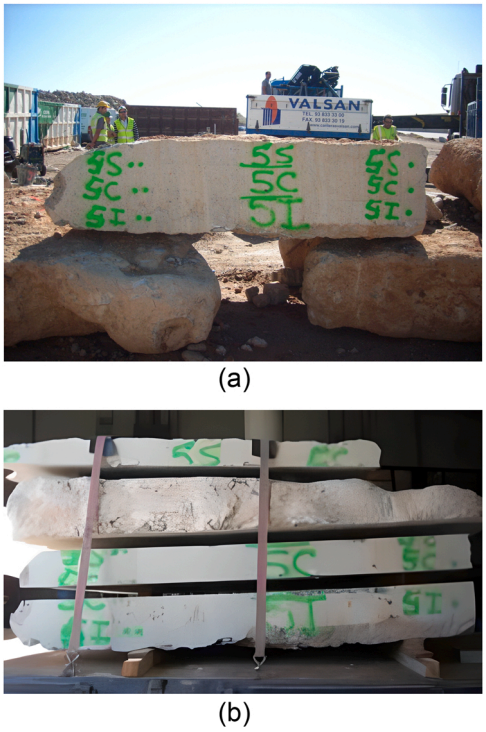

Fig. 7. a) Nomenclature of the walls, b) Transfer of the slabs to LTE.

Table 2
Standards and test methodologies applied.

Core sample type	Property	Standard/Method	Number of specimens tested
CCZ and CCY	Compressive strength (f_c)	UNE-EN 12390-3 [62]	72
	Modulus of elasticity (E_c)	UNE-EN 12390-13 [63]	72
	Amount (C_f) and orientation of steel fibers	Modified Inductive Method [64]	32
PC	Flexural tensile strength ($f_{ct,fl}$) and residual flexural strength (f_R)	EN 14651 [65]	18
	Amount (C_f) and orientation of steel fibers	Inductive Method [66]	46

The amount (C_f) and orientation of the steel fibers were characterized using cubic samples by means of the magnetic induction method, as described in [66]. This non-destructive method is based on the measures of the increments in inductance, due to the steel fibers inside the concrete. These increments depend on the C_f and on the type of steel of the fibers, since these steel fibers have some ferromagnetic properties and causes an alteration in the properties of the uniform magnetic field. An impedance analyzer (HP-4192) was used, with an error below 5%. For the cylindrical samples, the test was performed according to the method given in [64].

(a)

(b)

(c)

Fig. 8. a) Forklift, b) Distribution beam and support trestles, c) Neoprene.

2.4.2. Slabs obtained from the foundation walls

The elements tested were 18 slabs of variable geometry, 3 for each of the 6 walls. 9 of the slabs were made of fiber-reinforced concrete (those corresponding to walls 2, 5 and 6), while the remaining 9 were made of plain concrete (walls 1, 3 and 4); all the walls were made of concrete with recycled aggregates.

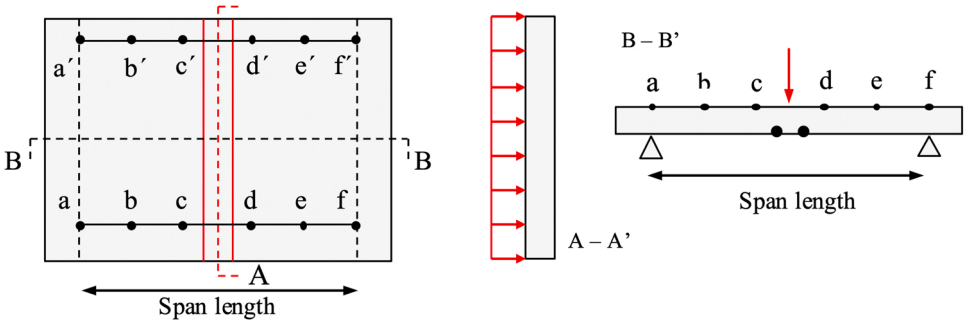

Fig. 9. LDVT's layout on the slabs.

The configuration of the test carried out consists of a simply supported configuration and a linear load applied onto the center span section through a steel spread beam of 2000 mm in length and 300 mm of flange width. To ensure a stable and even contact between slab and support trestles, and between the slab and the distribution beam, neoprene bands 200 mm wide and 20 mm thick were placed as shown in Fig. 8.

Fourteen linear variable displacement transducers (LVDTs) were used to record the vertical displacements of the slab and the evolution of cracks during the test. Twelve of these transducers were installed on an isolated auxiliary aluminum frame to measure the vertical displacements across the top part of the slabs, as illustrated in Fig. 9 and Fig. 10. The 2 remaining LVDTs were adhered to the side faces of the plate.

An initial preload of between 3.0 and 5.0 kN was applied to verify that the load was distributed correctly throughout the width of the slab. Once that point was reached, a control for the displacement approach was established to constantly maintain 0.25 mm/min. Once the load exceeded 20 kN, it the displacement velocity of the press was doubled increased. For FRC slabs, the test was stopped when a crack width of 5 mm was reached. For plain concrete elements, the test was stopped after cracking as no noticeable residual bearing capacity was observed. Fig. 11 presents the general test setup for the case of slab 4 S.

3. Results and discussion

3.1. Material

3.1.1. Physical and mechanical properties

Table 3 gathers the mean values and the coefficients of variation (CV expressed as percentages in parenthesis) of the density (δ), compressive strength (f_{cm}), modulus of elasticity (E_{cm}), flexural tensile strength ($f_{ctm,fl}$) and residual flexural tensile strengths (f_{R1m} and f_{R3m}, for crack mounts openings of 0.5 and 2.5 mm, respectively), for each wall and dosage.

The mean compressive strength characterized from the cored specimens resulted to be superior to 38 N/mm^2 (target value) for all concretes produced, except for the concrete FR-RA/12–35a, which exhibited an f_{cm} of 36.3 N/mm^2 (4% below). The residual flexural strength values derived from testing notched beam tests (following the [65]) resulted to range from 0.6 to 0.8 N/mm^2 and from 0.4 to 0.6 N/mm^2 for f_{R1} and f_{R3}, respectively. These magnitudes are low –and aligned with low amount of fibers– used according to the criteria stablished within the *fib* Model Code 2010 [67] for FRCs and these would not be sufficient to replace traditional steel longitudinal rebars. Nevertheless, it must be remarked that, in this pilot case, fibers were meant to replace skin reinforcement and to guarantee a minimum ductility in case of these panels cracked during service –situation very unlikely since the bending forces estimated were far below the cracking bending moment of the wall cross-section.

In the results, the average values of compressive strength exceed, for all the dosages, the minimum of 20 N/mm^2 required by the majority of standards for structural unreinforced concrete applications and the value of 25 N/mm^2 for reinforced concrete. Regarding the tensile strength results, the values vary between 2.63 and 3.35 N/mm^2; in contrast to compressive strength requirements, the recommendations usually do not establish a lower limit on the value of tensile strength, given that the reinforced-concrete structures are designed to permit controlled cracking of the concrete.

3.1.2. Content and orientation of fibers

Fig. 12 shows the results related to the orientation of steel fibers in the three foundation walls obtained using the inductive method [66] on 46 cubic cores with 150 mm-edge produced from the 18 prismatic cores previously tested for flexural stress (6 for each FRC dosage), following the cutting plan described above, in Section 2.3.1. The criterion used to identify the orientation and direction of the fibers was the following: axis 1 is the vertical axis (Z), axis 2 is the short (thickness) horizontal axis (Y) and axis 3 is the long (width) horizontal axis (X), as stated in Fig. 6.

The percentage of fibers oriented vertically (axis 1) increases in the three cases analyzed with respect to the results obtained with the specimens molded at the plant and at the laboratory [57], where approximately 70–80% of the fibers were oriented in the horizontal plane and 20–25% remain oriented in the vertical axis. This difference is due to the construction procedure used, as it influences the distribution and orientation of the fibers within the structural element [61], which increases the proportion of vertically oriented

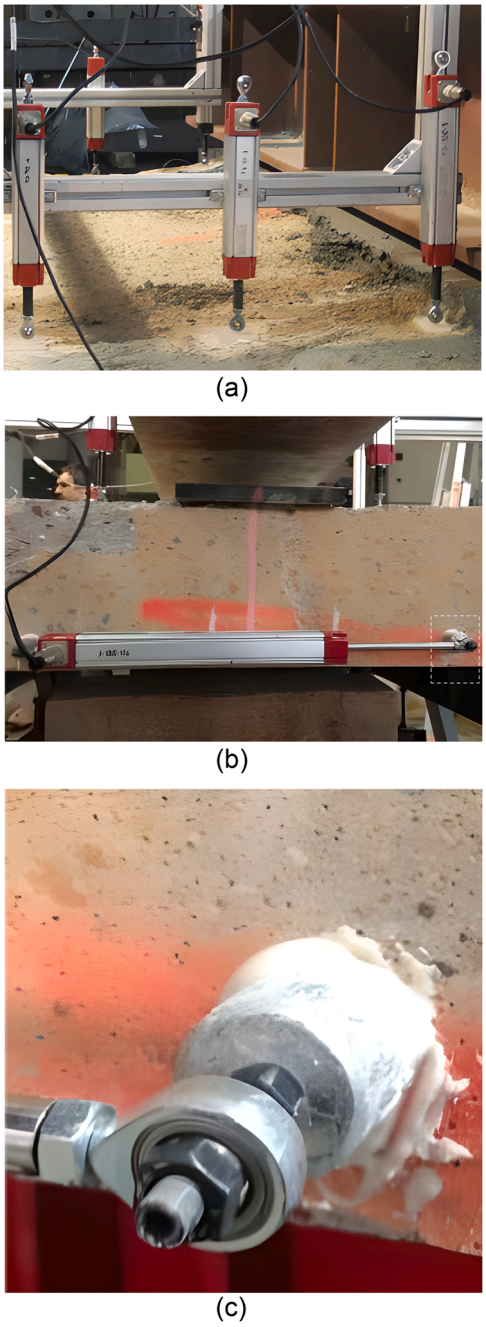

Fig. 10. a) and b) LVDTs placement, c) Detail of the X60 adhesive.

fibers.

In this regard, as [68,69] stated, steel fibers tend to orient perpendicular to the direction of flow and parallel to the formwork due to a wall effect. In the case of foundation walls, the flow direction of the concrete is predetermined to be vertical. As the self-compacting concrete flows freely and fills the excavated trench, the final arrangement of the fibers depends on their ability to rotate along the sections traveled, from the end of the tremie pipe to their final position. Therefore, the position and orientation of the fibers within the wall depends fundamentally on three factors:

- Consistency of the concrete: the more liquid the concrete is, the lower the resistance to flow and the fibers will have greater rotation and orientation ability depending on the direction of flow.
- Fiber geometry: the longer the fiber is, the lower the ability to rotate, and a greater proportion of fibers will be arranged vertically.

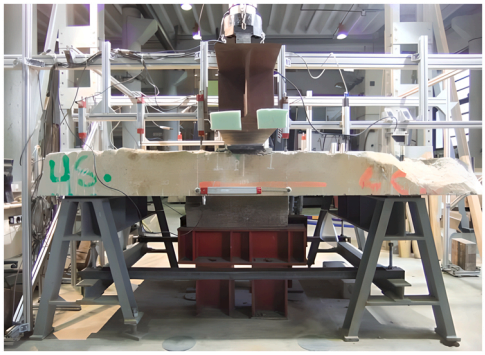

Fig. 11. Test setup (slab 4S).

Table 3
Results of the physical and mechanical characterization of the extracted cores.

Wall	Dosage	Density (g/cm^3)	f_{cm} (MPa)	E_{cm} (GPa)	$f_{ctm,fl}$ (MPa)	f_{R1m} (MPa)	f_{R3m} (MPa)
1	RA/SCC 20	2.1 (0.5)	42.4 (12.9)	25.5 (5.8)	3.1 (9.8)	–	–
2	FR-RA/SCC 12–35b	2.1 (0.2)	45.9 (5.4)	27.2 (4.2)	3.4 (10.8)	0.6	0.4
3	NA/SCC 12	2.3 (0.4)	45.2 (18.2)	34.4 (2.4)	3.1 (7.6)	–	–
4	RA/SCC 20 +I	2.1 (0.9)	39.7 (11.0)	26.1 (2.8)	3.2 (8.4)	–	–
5	FR-RA/12–35a	2.1 (0.5)	36.6 (6.9)	21.3 (3.5)	2.6 (14.3)	0.8	0.6
6	FR-RA/SCC 20–50	2.2 (0.4)	46.4 (5.2)	29.1 (2.5)	3.3 (8.9)	0.8	0.6

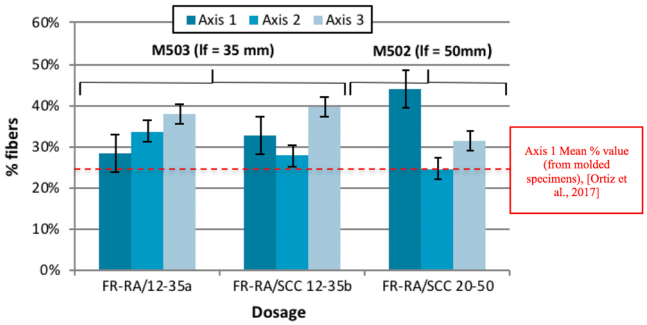

Fig. 12. Fiber orientation in the walls (data: 150 mm-edge cubic core samples).

- Wall dimensions: the larger the wall, the further the fiber must travel, and therefore the more likely it will rotate.

This has consequences, from a structural standpoint, on the post-cracking behavior of fiber-reinforced concrete slabs [70]. In any case, the results presented in Fig. 12 allow stating that the fibers are rather distributed 3-dimensionally as the percentages of fibers aligned along each axis ranges between 20% and 40%, this indicating that there are no preferential planes. The latter is beneficial in terms of control of cracks induced by shrinkage and temperature at early ages since this type of cracks use to appear randomly and without a pre-established direction. This makes the fibers oriented 3-dimensionally to be more effective as reinforcement for controlling this type of cracks.

It is worth mentioning, that for the FR-RA/12–35a mix (even though it cannot be considered as SCC) it can be observed an increment of the fibers aligned in the Y direction (short horizontal axis), compared to vertical direction (axis Z). This can be owing to the major resistance to flow and the movement of the fibers since this mix presented difficulties in meeting the self-compacting requirements, as explained before in Section 2.1.

Finally, the amount of fibers assessed by means the inductive test performed on the 46 cubic specimens cut from the walls ranged

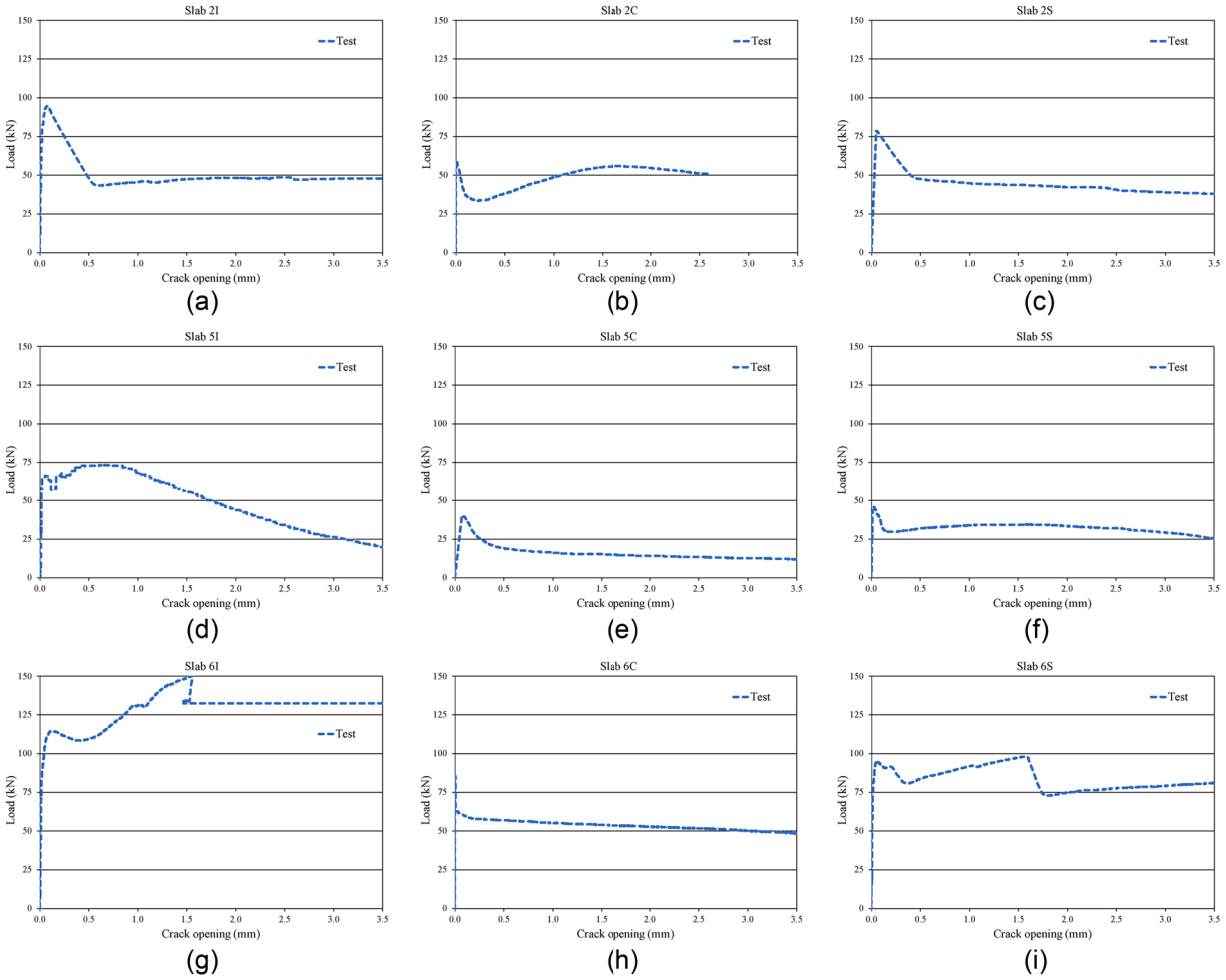

Fig. 13. Diagram P-w. Slabs HRF a) 2I, b) 2 C, c) 2 S, d) 5I, e) 5 C, f) 5 S, g) 6I, h) 6 C and i) 6S.

between 13.4 and 21.2 kg/m^3, with an average of 18.1 kg/m^3 and CoV of 14%. A similar statistical pattern of the fiber distribution was observed for those walls reinforced with steel fibers and, therefore, no significant influence of the concrete consistency and the aggregates nature/origin on the fiber distribution was observed.

3.2. *Mechanical performance of the tested slabs*

The applied force (F) – crack opening (w) relationships derived from the real-scale bending tests are presented in Fig. 13. It must be remarked that the variability observed was expected due to the irregular geometry of the slabs, which in any case is that found in the real structure and, thus, the representative of the mechanical response of the wall.

The cracking load (F_{cr}) ranged from 59.2 to 94.7 kN (slabs type 2), from 40.1 to 66.4 kN (type 5) and from 85.2 to 114.7 kN (type 6). The variability of F_{cr} must be attributed to the variability of the: (1) thickness (CoV up to 20%) of the cracked sections and (2) $f_{ctm,fl}$ (see Table 3), which ranged between 2.6 and 3.4 N/mm^2 (CoV of 9%), the former being the parameter that governs the variability of F_{cr} – depends quadratically of h and linearly of $f_{ct,fl}$ –.

As per post-cracking response of the fiber reinforced concrete slabs, a deflection softening behavior, without a brittle failure after cracking, due to the effective contribution of fibers across the cracked section can be observed. A ratio $F_{2.5}/F_{cr}$ superior to 0.5 was achieved for the slabs type 2 and 6, $F_{2.5}$ being the force for a w = 2.5 mm. This ratio was imposed during the design of the FRC walls in order to avoid a fragile response of slabs after cracking. In this regard, it must be highlighted that the reinforcement of these walls responded to minimum requirements for shrinkage and temperature cracking and, hence, this was replaced by steel macrofibers (see Table 1).

This criterion is aligned with the *fib* Model Code 2010 [67] requirements per FRC ductility: (1) $f_{R1k}/f_{LOPk} > 0.4$ and (2) $f_{R3k}/f_{R1k} > 0.5$ and, consequently, $f_{R3k}/f_{LOPk} > 0.2$. As f_{LOP} and f_{R3} are directly related with F_{cr} and $F_{2.5}$, respectively, it was found appropriate –and on the safe side– to equivalently impose $F_{2.5}/F_{cr} > 0.5$.

4. Conclusions

A pilot experience of using recycled-aggregates (RA), replacing 100% of the natural coarse aggregates, for producing steel fiber reinforced self-compacting concrete (FR-SCC-RA) oriented to the construction of foundation walls was presented in this paper. An experimental program oriented to characterize the mechanical performance of FR-SCC-RA and foundation walls made of this material was carried out and the results are presented and discussed herein. The following conclusions can be stated:

- The compressive strength (f_c) and modulus of elasticity (E_c) of the concrete produced with 100% of RA was found compatible (and sufficient) with the strength and stiffness that these types of walls are required for service and ultimate limit states.
- The use of steel macrofibers for replacing the skin reinforcement proved to be a suitable alternative as no cracks were observed. Moreover, the residual post-cracking strength of the slabs (cut from the wall) obtained from the real-scale bending tests was proven adequate to avoid fragile response after cracking.

Based on the abovementioned, it can be stated that FR-SCC-RA can be an attractive –from both technical and sustainable perspectives– to traditional reinforced concrete (with natural aggregates) for this structural typology. Nevertheless, this consisted in a pilot case mean to confirm the adequacy of the material for the production of the walls and its sufficient load bearing capacity, and further research has to be conducted in order to establish requirements on the fresh state properties, structural design and durability.

Declaration of Competing Interest

The authors declare that they have no known competing financial interests or personal relationships that could have appeared to influence the work reported in this paper.

Data Availability

No data was used for the research described in the article.

Acknowledgments

The authors would like to thank the Agency for Management of University and Research Grants (AGAUR), Barcelona, Spain and the company ESCOFET 1886, S.A., Barcelona, Spain, for the economic support within the Industrial Doctorate Programme of Dr. Francisco Mena. This study was also fund by the Spanish Ministry of Science and Innovation under the scope of project CREEF (PID2019-108978RB-C32). Likewise, the authors wish to thank the Structure Technology Laboratory Luis Agulló Lab Staff, belonging to Barcelona Tech, Spain.

References

[1] T. Park, Application of construction and building debris as base and subbase materials in rigid pavement, J. Transp. Eng. 129 (2003) 558–563, https://doi.org/10.1061/(ASCE)0733-947X(2003)129:5(558).
[2] J.R. Jiménez, F. Agrela, J. Ayuso, M. López, Estudio comparativo de los áridos reciclados de hormigón y mixtos como material para sub-bases de carreteras, Mater. Constr. 61 (2011) 289–302, https://doi.org/10.3989/mc.2010.54009.
[3] F. Agrela, A. Barbudo, A. Ramírez, J. Ayuso, M.D. Carvajal, J.R. Jiménez, Construction of road sections using mixed recycled aggregates treated with cement in Malaga, Spain, Resour. Conserv. Recycl. 58 (2012) 98–106, https://doi.org/10.1016/j.resconrec.2011.11.003.
[4] R. Herrador, P. Pérez, L. Garach, J. Ordóñez, Use of recycled construction and demolition waste aggregate for road course surfacing, J. Transp. Eng. 138 (2012) 182–190, https://doi.org/10.1061/(ASCE)TE.1943-5436.0000320.
[5] L. Ferrara, High performance fibre reinforced cementitious composites: six memos for the XXI century societal and economical challenges of civil engineering, Case Stud. Constr. Mater. 10 (2019), e00219, https://doi.org/10.1016/j.cscm.2019.e00219.
[6] Comisión Permanente del Hormigón (CPH), Structural Code, Ministerio de Presidencia, Relaciones con las Cortes y Memoria Democrática, Gobierno de España, Madrid, 2021.
[7] I. Josa, N. Tošić, S. Marinković, A. de la Fuente, A. Aguado, Sustainability-oriented multi-criteria analysis of different continuous flight auger piles, Sustainability 13 (2021), https://doi.org/10.3390/su13147552.
[8] Asociación Española de Gestores de Residuos de Construcción y Demolición, Guía Española de Áridos Reciclados procedentes de Residuos de Construcción y Demolición, Spain, 2012. ⟨https://www.btbab.com/wp-content/uploads/documentos/legislacion/Guia_Gerd_2012.pdf⟩.
[9] S.P. de G.A. IHOBE, Usos de áridos reciclados mixtos procedentes de Residuos de Construcción y Demolición, Investigación prenormativa, Departamento de Medio Ambiente, Planificación Territorial, Agricultura y Pesca. Gobierno Vasco, Bilbao, Spain, 2011.
[10] A.D. Tegguer, Determining the water absorption of recycled aggregates utilizing hydrostatic weighing approac, Constr. Build. Mater. 27 (2012) 112–116, https://doi.org/10.1016/j.conbuildmat.2011.08.018.
[11] J. García, D. Rodríguez, A. Juan, J.M. Morán, M.I. Guerra, Pre-saturación de los áridos reciclados procedentes de residuos de construcción y demolición para la fabricación de hormigones eco-eficientes, in: Mem. VI Congr. Int. Estruct. ACHE, ACHE (Asociación Científico-Técnica del Hormigón Estructural), Madrid, 2014.
[12] N. Klein, A. Aguado, B. Toralles-Carbonari, L.V. Real, Prediction of the water absorption by aggregates over time: modelling through the use of value function and experimental validation, Constr. Build. Mater. 69 (2014) 213–220, https://doi.org/10.1016/j.conbuildmat.2014.07.048.
[13] M. Etxeberria, M. Konoiko, C. Garcia, M.Á. Perez, Water-washed fine and coarse recycled aggregates for real scale concretes production in Barcelona, Sustainability 14 (2022), https://doi.org/10.3390/su14020708.
[14] P. Kathirvel, G. Murali, N.I. Vatin, S.R. Abid, Experimental study on self compacting fibrous concrete comprising magnesium sulphate solution treated recycled aggregates, Materials 15 (2022), https://doi.org/10.3390/ma15010340.
[15] P. Mehrabi, M. Shariati, K. Kabirifar, M. Jarrah, H. Rasekh, N.T. Trung, A. Shariati, S. Jahandari, Effect of pumice powder and nano-clay on the strength and permeability of fiber-reinforced pervious concrete incorporating recycled concrete aggregate, Constr. Build. Mater. 287 (2021), 122652, https://doi.org/10.1016/j.conbuildmat.2021.122652.

[16] A. Toghroli, P. Mehrabi, M. Shariati, N.T. Trung, S. Jahandari, H. Rasekh, Evaluating the use of recycled concrete aggregate and pozzolanic additives in fiber-reinforced pervious concrete with industrial and recycled fibers, Constr. Build. Mater. 252 (2020), 118997, https://doi.org/10.1016/j.conbuildmat.2020.118997.
[17] Toghroli Ali, Shariati Mahdi, Sajedi Fathollah, Ibrahim Zainah, Koting Suhana, Mohamad Edy Tonnizam, Khorami Majid, A review on pavement porous concrete using recycled waste materials, Smart Struct. Syst. 22 (2018) 433–440, https://doi.org/10.12989/SSS.2018.22.4.433.
[18] F. Xu, X. Lin, A. Zhou, Q. Liu, Effects of recycled ceramic aggregates on internal curing of high performance concrete, Constr. Build. Mater. 322 (2022), 126484, https://doi.org/10.1016/j.conbuildmat.2022.126484.
[19] P.B. Cachim, Mechanical properties of brick aggregate concrete, Constr. Build. Mater. 23 (2009) 1292–1297, https://doi.org/10.1016/j.conbuildmat.2008.07.023.
[20] J.B. Bazaz, M. Khayati, Properties and performance of concrete made with recycled low-quality crushed brick, J. Mater. Civ. Eng. 24 (2012) 330–338, https://doi.org/10.1061/(ASCE)MT.1943-5533.0000385.
[21] A. Rao, Experimental Investigation on Use of Recycled Aggregates in Mortar and Concrete, Thesis, Departament of Civil Engineering, Indian Institute of Technology Kampur, 2005.
[22] M. Etxeberria, A.R. Marí, E. Vázquez, Recycled aggregate concrete as structural material, Mater. Struct. 40 (2007) 529–541, https://doi.org/10.1617/s11527-006-9161-5.
[23] S.C. Kou, S.C. Poon, Properties of self-compacting concrete prepared with coarse and fine recycled concrete aggregates, Cem. Concr. Compos. 31 (2009) 622–627, https://doi.org/10.1016/j.cemconcomp.2009.06.005.
[24] A. Gonzalez-Corominas, M. Etxeberria, Properties of high performance concrete made with recycled fine ceramic and coarse mixed aggregates, Constr. Build. Mater. 68 (2014) 618–626, https://doi.org/10.1016/j.conbuildmat.2014.07.016.
[25] M.C. Rao, S.K. Bhattacharyya, S.V. Barai, Influence of field recycled coarse aggregate on properties of concrete, Mater. Struct. 44 (2011) 205–220, https://doi.org/10.1617/s11527-010-9620-x.
[26] J. Xiao, J. Li, C. Zhang, Mechanical properties of recycled aggregate concrete under uniaxial loading, Cem. Concr. Res. 35 (2005) 1187–1194, https://doi.org/10.1016/j.cemconres.2004.09.020.
[27] S.C. Kou, C.S. Poon, Mechanical properties of 5-year old concrete prepared with recycled aggregates obtained from three different sources, Mag. Concr. Res. 60 (2008) 57–64, https://doi.org/10.1680/macr.2007.00052.
[28] J.B. Li, Study on Mechanical Behavior of Recycled Aggregate Concrete, Master Thesis, Tongji University, 2004.
[29] I. Martínez-Lage, F. Martínez-Abella, C. Vázquez-Herrero, J.L. Pérez-Ordóñez, Properties of plain concrete made with mixed recycled coarse aggregate, Constr. Build. Mater. 37 (2012) 171–176, https://doi.org/10.1016/j.conbuildmat.2012.07.045.
[30] O. Pons, M.M. Casanovas-Rubio, J. Armengou, A. de la Fuente, Sustainability-driven decision-making model: case study of fiber-reinforced concrete foundation piles, J. Constr. Eng. Manag. 147 (2021), 04021116, https://doi.org/10.1061/(ASCE)CO.1943-7862.0002073.
[31] A.C.P. Santos, J.A. Ortiz-Lozano, N. Villegas, A. Aguado, Experimental study about the effects of granular skeleton distribution on the mechanical properties of self-compacting concrete (SCC), Constr. Build. Mater. 78 (2015) 40–49, https://doi.org/10.1016/j.conbuildmat.2015.01.006.
[32] A. Alrawashdeh, O. Eren, Mechanical and physical characterisation of steel fibre reinforced self-compacting concrete: Different aspect ratios and volume fractions of fibres, Results Eng. 13 (2022), 100335, https://doi.org/10.1016/j.rineng.2022.100335.
[33] S. Meng, C. Jiao, X. Ouyang, Y. Niu, J. Fu, Effect of steel fiber-volume fraction and distribution on flexural behavior of Ultra-high performance fiber reinforced concrete by digital image correlation technique, Constr. Build. Mater. 320 (2022), 126281, https://doi.org/10.1016/j.conbuildmat.2021.126281.
[34] D. Akhmetov, S. Akhazhanov, A. Jetpisbayeva, Y. Pukharenko, Y. Root, Y. Utepov, A. Akhmetov, Effect of low-modulus polypropylene fiber on physical and mechanical properties of self-compacting concrete, Case Stud. Constr. Mater. 16 (2022), e00814, https://doi.org/10.1016/j.cscm.2021.e00814.
[35] A. De la Fuente, A. Blanco, J. Armengou, A. Aguado, Sustainability based-approach to determine the concrete type and reinforcement configuration of TBM tunnel linings. Case study: extension line to Barcelona Airport T1, Tunn. Undergr. Space Technol. 61 (2017) 179–188, https://doi.org/10.1016/j.tust.2016.10.008.
[36] A. De la Fuente, M. del M. Casanovas-Rubio, O. Pons, J. Armengou, Sustainability of column-supported RC slabs: fiber reinforcement as an alternative, J. Constr. Eng. Manag. 145 (2019), 04019042, https://doi.org/10.1061/(ASCE)CO.1943-7862.0001667.
[37] N.T. Nguyen, T.-T. Bui, Q.-B. Bui, Fiber reinforced concrete for slabs without steel rebar reinforcement: Assessing the feasibility for 3D-printed individual houses, Case Stud. Constr. Mater. 16 (2022), e00950, https://doi.org/10.1016/j.cscm.2022.e00950.
[38] A.K.L.L. Nzambi, J.B. Ntuku, D.R.C. de Oliveira, Empirical equations for flexural residual strengths in concrete with low volumetric fractions of hook-end steel fiber, Eng. Rep. N./a (2021), e12490, https://doi.org/10.1002/eng2.12490.
[39] J.A.O.-L. Julian Carrillo, Juan G. Rueda-Bayona, Indirect tensile behavior of hooked-end steel fiber- reinforced concrete under double-punch tests, Acids Mater. J. 118 (2021), https://doi.org/10.14359/51732932.
[40] J. Ahmad, O. Zaid, F. Aslam, R. Martínez-García, Y.M. Alharthi, M. Hechmi, E.I. Ouni, R.F. Tufail, I.A. Sharaky, Mechanical properties and durability assessment of nylon fiber reinforced self-compacting concrete, J. Eng. Fibers Fabr. 16 (2021), https://doi.org/10.1177/15589250211062833.
[41] M.Tolga Cogurcu, Investigation of mechanical properties of red pine needle fiber reinforced self-compacting ultra high performance concrete, Case Stud. Constr. Mater. 16 (2022), e00970, https://doi.org/10.1016/j.cscm.2022.e00970.
[42] A. Meda, G.A. Plizzari, P. Riva, Fracture behavior of SFRC slabs on grade, Mater. Struct. 37 (2004) 405–411, https://doi.org/10.1007/BF02479637.
[43] Alberto Meda, Giovanni A. Plizzari, New design approach for steel fiber-reinforced concrete slabs-on-ground based on fracture mechanics, Acids Struct. J. 101 (2004), https://doi.org/10.14359/13089.
[44] O.E. Cakir, F. Cetisli, Behavior of steel fiber reinforced concrete panels under surface pressure, Sustainability 14 (2022), https://doi.org/10.3390/su14010298.
[45] A. De la Fuente, P. Pujadas, A. Blanco, A. Aguado, Experiences in Barcelona with the use of fibres in segmental linings, Tunn. Undergr. Space Technol. 27 (2012) 60–71, https://doi.org/10.1016/j.tust.2011.07.001.
[46] A. De la Fuente, R.C. Escariz, A.D. De Figueiredo, C. Molins, A. Aguado, A new design method for steel fibre reinforced concrete pipes, Constr. Build. Mater. 30 (2012) 547–555, https://doi.org/10.1016/j.conbuildmat.2011.12.015.
[47] A. De la Fuente, A. Aguado, C. Molins, J. Armengou, Innovations on components and testing for precast panels to be used in reinforced earth retaining walls, Constr. Build. Mater. 25 (2011) 2198–2205, https://doi.org/10.1016/j.conbuildmat.2010.11.003.
[48] A. Caratelli, A. Meda, Z. Rinaldi, P. Romualdi, Structural behaviour of precast tunnel segments in fiber reinforced concrete, Tunn. Undergr. Space Technol. 26 (2011) 284–291, https://doi.org/10.1016/j.tust.2010.10.003.
[49] A.M. Luca, G. Sorelli, Giovanni A. Plizzari, Steel fiber concrete slabs on ground: a structural matter, Acids Struct. J. 103 (2006), https://doi.org/10.14359/16431.
[50] D. Fall, J. Shu, R. Rempling, K. Lundgren, K. Zandi, Two-way slabs: experimental investigation of load redistributions in steel fibre reinforced concrete, Eng. Struct. 80 (2014) 61–74, https://doi.org/10.1016/j.engstruct.2014.08.033.
[51] F. Mora Apablaza, Distribucion y orientacion de fibras en dovelas, aplicando el ensayo barcelona, PhD Thesis, Universitat Politècnica de Catalunya (UPC), 2008. ⟨https://dialnet.unirioja.es/servlet/tesis?codigo=259471⟩ (accessed July 27, 2021).
[52] S. Aidarov, F. Mena, A. de la Fuente, Structural response of a fibre reinforced concrete pile-supported flat slab: full-scale test, Eng. Struct. 239 (2021), 112292, https://doi.org/10.1016/j.engstruct.2021.112292.
[53] H.M. Adnan, A.O. Dawood, Strength behavior of reinforced concrete beam using re-cycle of PET wastes as synthetic fibers, Case Stud. Constr. Mater. 13 (2020), e00367, https://doi.org/10.1016/j.cscm.2020.e00367.
[54] D. Gao, W. Zhu, D. Fang, J. Tang, H. Zhu, Shear behavior analysis and capacity prediction for the steel fiber reinforced concrete beam with recycled fine aggregate and recycled coarse aggregate, Structures 37 (2022) 44–55, https://doi.org/10.1016/j.istruc.2021.12.075.
[55] N. Nassif, W. Zeiada, G. Al-Khateeb, S. Haridy, S. Altoubat, Assessment of punching shear strength of fiber-reinforced concrete flat slabs using factorial design of experiments, Jordan J. Civ. Eng. 16 (2022) 2022.

[56] N. Kachouh, T. El-Maaddawy, H. El-Hassan, B. El-Ariss, Shear response of recycled aggregates concrete deep beams containing steel fibers and web openings, Sustainability 14 (2022), https://doi.org/10.3390/su14020945.
[57] J.A. Ortiz, A. de la Fuente, F. Mena Sebastia, I. Segura, A. Aguado, Steel-fibre-reinforced self-compacting concrete with 100% recycled mixed aggregates suitable for structural applications, Constr. Build. Mater. 156 (2017) 230–241, https://doi.org/10.1016/j.conbuildmat.2017.08.188.
[58] B. Chiaia, A.P. Fantilli, P. Vallini, Minimum reinforcement and fiber contribution in tunnel linings: the Italian experience, in: Proc. Fourth Int. Struct. Eng. Constr. Conf., Taylor & Francis Group, Melbourne, 2007: pp. 365–370. https://doi.org/porto.polito.it/id/eprint/1660903.
[59] A.P. Fantilli, B. Chiaia, A. Gorino, Unified approach for minimum reinforcement of concrete beams, Acids Struct. J. 113 (2016) 1107–1116, https://doi.org/10.14359/51688927.
[60] A. Orbe, J. Cuadrado, R. Losada, E. Rojí, Framework for the design and analysis of steel fiber reinforced self-compacting concrete structures, Constr. Build. Mater. 35 (2012) 676–686, https://doi.org/10.1016/j.conbuildmat.2012.04.135.
[61] A. Orbe Mateo, Optimización del Uso de Hormigones Autocompactantes Reforzados con Fibras de Acero en Aplicaciones Convencionales de Resistencias Moderadas, PhD Thesis, Universidad del País Vasco, 2013. ⟨https://addi.ehu.es/handle/10810/11156⟩ (accessed August 2, 2021).
[62] UNE-EN 12390–3:2020, Testing hardened concrete - Part 3: Compressive strength of test specimens, 2020. ⟨https://www.normadoc.com/english/une-en-12390–3-2020.html⟩ (accessed August 2, 2021).
[63] UNE-EN 12390–13:2014, Testing hardened concrete - Part 13: Determination of secant modulus of elasticity in compression, 2014. ⟨https://www.une.org/encuentra-tu-norma/busca-tu-norma/norma/?c=N0053157⟩ (accessed August 2, 2021).
[64] S.H.P. Cavalaro, R. López-Carreño, J.M. Torrents, A. Aguado, P. Juan-García, Assessment of fibre content and 3D profile in cylindrical SFRC specimens, Mater. Struct. 49 (2016) 577–595, https://doi.org/10.1617/s11527-014-0521-2.
[65] BSI, BS EN 14651:2005+A1:2007 - Test method for metallic fibre concrete. Measuring the flexural tensile strength (limit of proportionality (LOP), residual) (British Standard), BSI: British Standards Institution, 2007. ⟨https://standards.globalspec.com/std/1086710/BS%20EN%2014651⟩ (accessed September 2, 2020).
[66] J.M. Torrents, A. Blanco, P. Pujadas, A. Aguado, P. Juan-García, M.A. Sánchez-Moragues, Inductive method for assessing the amount and orientation of steel fibers in concrete, Mater. Struct. 45 (2012) 1577–1592, https://doi.org/10.1617/s11527-012-9858-6.
[67] The International Federation for Structural Concrete (fib), The fib Model Code for Concrete Structures 2010, Wiley-VCH Verlag GmbH & Co., KGaA, Weinheim, German, 2013. https://doi.org/10.1002/9783433604090.
[68] A. Blanco Alvarez, Characterization and modelling of SFRC elements, PhD Thesis, Universitat Politècnica de Catalunya (UPC), 2013. ⟨https://dialnet.unirioja.es/servlet/tesis?codigo=97127⟩ (Accessed July 27, 2021).
[69] A. Blanco, P. Pujadas, A. de la Fuente, S.H.P. Cavalaro, A. Aguado, Assessment of the fibre orientation factor in SFRC slabs, Compos. Part B Eng. 68 (2015) 343–354, https://doi.org/10.1016/j.compositesb.2014.09.001.
[70] S. Khan, L. Qing, I. Ahmad, R. Mu, M. Bi, Investigation on fracture behavior of cementitious composites reinforced with aligned hooked-end steel fibers, Materials 15 (2022), https://doi.org/10.3390/ma15020542.